(Inverse) magnetic catalysis and phase transition in QCD

Jens O. Andersen [1]

NTNU – Trondheim
Norwegian University of
Science and Technology

Theory Seminar ITP Wien, Monday October 6 2014.

[1] In collaboration with Anders Tranberg (University of Stavanger), William Naylor and Rashid Khan (NTNU),

PRD 85 065026 (2012), JHEP 1208 (2012) 002, JHEP 1404 (2014) 187.

Phase diagram of QCD

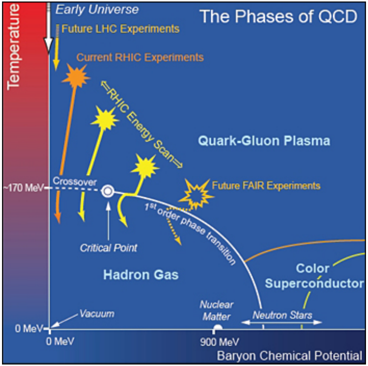

Hadronic matter in strong magnetic fields:

- Non-central heavy-ion collisions [2]

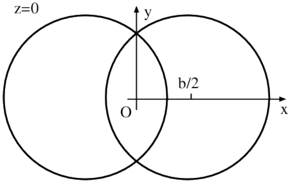

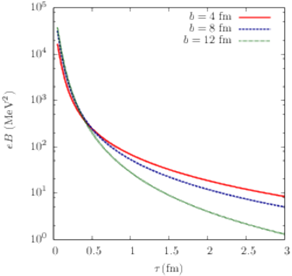

[2] Kharzeev, McLerran, and Warringa, Nucl. Phys. **A** 803 (2008) 227, Skokov, Illarianov, and Toneev, Int. J. Mod. Phys. **A** 24 (2009) 5925.

Hadronic matter in strong magnetic fields:

- Magnetars $B = 10^{10}$ T [3]

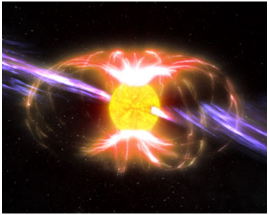

- Electroweak phase transition $B = 10^{19}$ T [4]

[3] Duncan and Thompson

[4] Vachaspati, Enqvist and Olesen. Rummukainen et. al.

Lattice, effective theories, and models

- Lattice (Buividovich et al, D'Elia et al , Endrődi et al, Bali et al.
- Bag model (Fraga and Palhares)
- Chiral perturbation theory (Agasian and Shushpanov, Agasian and Fedorov, JOA...)
- (Polyakov-loop extended) Nambu-Jona-Lasinio model (Mizher, Chernodub, and Fraga, Fukushima, Ruggieri and Gatto, Kashiwa...)
- (Polyakov loop extended) Linear sigma model with quarks (Skokov, JOA+Tranberg+Naylor)
- Holographic models (Preis, Rebhan, and Schmitt)
- Schwinger-Dyson (Bonnet et al.)

Some important questions:

- Critical temperature as a function of B
  - Chiral condensate increases with B at $T = 0$
- Splitting of chiral and deconfinement transition
  - Can be addressed by adding the Polyakov loop
- Phase diagram in a magnetic background
  - Does the magnetic field change the order of the transition? Position of critical endpoint?

Lagrangian and symmetries

$$
\begin{aligned}
\mathcal{L} \;=\; & \bar{\psi}\Big[\gamma_\mu\partial_\mu + g(\sigma - i\gamma_5\boldsymbol{\tau}\cdot\boldsymbol{\pi})\Big]\psi + \frac{1}{2}\Big[(\partial_\mu\sigma)^2 + (\partial_\mu\boldsymbol{\pi})^2\Big] \\
& + \frac{1}{2}m^2\Big[\sigma^2 + \boldsymbol{\pi}^2\Big] + \frac{\lambda}{24}\Big[\sigma^2 + \boldsymbol{\pi}^2\Big]^2 - h\sigma \,.
\end{aligned}
$$

- $O(4)$-symmetry broken to $O(3)$ by chiral condensate. Three Goldstone bosons (pions).
- Magnetic field breaks $SU(2)$ isopin symmetry. Only the neutral pion is a Goldstone mode.
- $\sigma^2 + \boldsymbol{\pi}^2 \to (\sigma^2 + \pi_0^2) + 2(\pi^+\pi^-)$ with two separate couplings.

Mean-field approximation

- Background and quantum field

$$\sigma \quad \rightarrow \quad \phi + \tilde{\sigma} \; .$$

- Omit bosonic quantum and thermal fluctuations. Large-N_c limit
- Effective potential

$$\begin{aligned}
\mathcal{F}_{0+1} &= \frac{1}{2}m^2\phi^2 + \frac{\lambda}{24}\phi^4 - h\phi - \mathrm{Tr}\log S^{-1} \; , \\
\mathrm{Tr}\log S^{-1} &= -\sum_f \mathrm{Tr}\log[i\gamma_\mu(P_\mu + q_f A_\mu) + m_q] \; , \\
m_q &= g\phi \; .
\end{aligned}$$

Mean-field approximation

- One-loop contribution

$$
\begin{aligned}
\mathcal{F}_1 &= -\sum\!\!\!\!\!\!\!\int_{\{P\}}^{B} \ln\left[P_0^2 + p_z^2 + M_B^2\right] \\
&= \frac{|q_f B|}{2\pi} \sum_{s,k,P_0} \int \frac{dp_z}{2\pi} \ln\left[P_0^2 + p_z^2 + m_q^2 + |q_f B|(2k+1-s)\right] . \\
\mathcal{F}_1^{T=0} &= \frac{|q_f B|}{2\pi} \sum_{s=\pm 1} \sum_{k=0}^{\infty} \int \frac{dp_z}{2\pi} \sqrt{p_z^2 + m_q^2 + |q_f B|(2k+1-s)} \\
&= -\frac{|q_f B|}{2\pi} \left(e^{\gamma_E}\Lambda^2\right)^{\epsilon} \Gamma(-1+\epsilon) \\
&\quad \times \sum_{s,k} \left[m^2 + |q_f B|(2k+1-s)\right]^{1-\epsilon} .
\end{aligned}
$$

Mean-field approximation

- Hurwitz zeta function:

$$\zeta(s,q) = \sum_{k=0}^{\infty}(k+q)^s$$

$$\begin{aligned}
F_1^{T=0} &= \frac{(q_fB)^2}{2\pi^2}\left(\frac{e^{\gamma_E}\Lambda^2}{2|q_fB|}\right)^{\epsilon}\Gamma(-1+\epsilon)\left[\zeta(-1+\epsilon,x_f)-\frac{1}{2}x_f\right] \\
&= \frac{1}{(4\pi)^2}\left(\frac{\Lambda^2}{2|q_fB|}\right)^{\epsilon}\Bigg[\left(\frac{2(q_fB)^2}{3}+m_q^4\right)\left(\frac{1}{\epsilon}+1\right) \\
&\quad -8(q_fB)^2\zeta^{(1,0)}(-1,x_f)-2|q_fB|m_q^2\ln x_f+\mathcal{O}(\epsilon)\Bigg]\,, \\
x_f &= \frac{m_q^2}{2|q_fB|}\,.
\end{aligned}$$

Mean-field approximation

- Renormalized one-loop effective potential

$$
\begin{aligned}
\mathcal{F}_{0+1} &= \frac{1}{2}B^2\left[1+N_c\sum_f\frac{4q_f^2}{3(4\pi)^2}\ln\frac{\Lambda^2}{|2q_fB|}\right]+\frac{1}{2}m^2\phi^2+\frac{\lambda}{24}\phi^4\\
&-\frac{N_c}{2\pi^2}\sum_f(q_fB)^2\left[\zeta^{(1,0)}(-1,x_f)+\frac{1}{2}x_f\ln x_f-\frac{1}{4}x_f^2\right.\\
&\left.-\frac{1}{2}x_f^2\ln\frac{\Lambda^2}{2|q_fB|}\right]-\frac{N_cT^2}{8\pi^2}\sum_f|q_fB|K_0^B(\beta m_q)\,.\\
K_0^B(\beta m) &= 8\sum_{s,k}\int_0^\infty\frac{dp_z\,p_z^2}{\sqrt{p_z^2+M_B^2}}\frac{1}{e^{\beta\sqrt{p_z^2+M_B^2}}+1}\,.
\end{aligned}
$$

Magnetic catalysis at $T = 0$

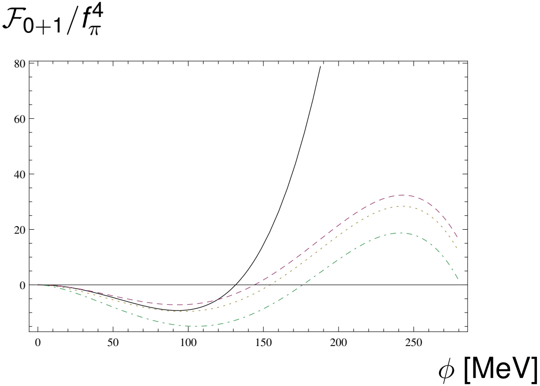

- One-loop effective potential unstable - need bosonic contribution to stabilize.
- By subtracting one-loop effective potential at $B = 0$, one avoids the instability.

Phase transition

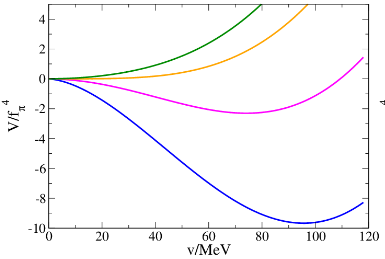

Figure: Effective potential in the chiral limit.

- Order of phase phase transition depends on treatment of vacuum fluctuations
- First-order vs crossover at the physical point.

Functional renormalization group

- Flow equation for the effective average action $\Gamma_k[\phi]$ that interpolates between the classical action S for $k = \Lambda$ and full quantum effective action $\Gamma_0[\phi]$ for $k = 0$ [5].

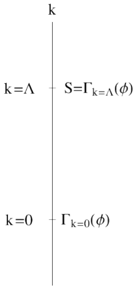

[5] Wetterich, *Nucl. Phys. B* **352** (1991) 529, Berges, Pawlowski, Schaefer and Wambach, Skokov...

Functional renormalization group

$$
\begin{aligned}
S[\phi] &\rightarrow S[\phi] + \frac{1}{2}\int \frac{d^dq}{(2\pi)^d}\phi(-q)R_k(q)\phi(q)\,, \\
\mathcal{Z}[J] &= \int \mathcal{D}\phi e^{-S[\phi]-\Delta S_k[\phi]+\int J\phi} \\
\Gamma_k[\phi] &= -\ln \mathcal{Z}_k + \int j\phi - \Delta S_k[\phi]
\end{aligned}
$$

- $R_k(q)$ satisfies various conditions to implement RG ideas:
  - Suppress momenta *pqk* and leave momenta $q > k$ unchanged.
  - $R_{k=0}(q) = 0$ and $R_{k=\Lambda}(q) = \infty$.

- Flow equation for $\Gamma_k[\phi]$

$$\partial_k \Gamma_k[\phi] = \frac{1}{2}\mathrm{Tr}\left[\partial_k R_k(q)\left[\Gamma_k^{(2)} + R_k(q)\right]^{-1}\right] + \text{term for fermions}\,.$$

- Flow equation is exact.
- Feynman diagram for flow equation

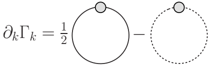

Functional renormalization group

- Cannot solve flow equation exactly. Derivative expansion:

$$
\begin{aligned}
\Gamma_k[\phi] &= \int_0^\beta d\tau \int d^3x \left\{ \frac{1}{2} Z_k^{(1)} \left[(\nabla\sigma)^2 + (\nabla\boldsymbol{\pi})^2 \right] \right. \\
&+ \frac{1}{2} Z_k^{(2)} \left[(\partial_0\sigma)^2 + (\partial_0\boldsymbol{\pi})^2 \right] + U_k(\phi) + Z_k^{(3)} \bar{\psi}\gamma_0\partial_0\psi \\
&\left. + Z_k^{(4)} \bar{\psi}\gamma_i\partial_i\psi + g_k\bar{\psi}\left[\sigma - i\gamma_5\boldsymbol{\tau}\cdot\boldsymbol{\pi}\right]\psi + \ldots \right\} ,
\end{aligned}
$$

- Local-potential approximation (LPA): $Z_k^{(i)} = 1$ yields equation for effective potential $U_k[\phi]$.
- Beyond LPA: calculate anomalous dimensions.

Functional renormalization group

$$
\begin{aligned}
\partial_k U_k \;=\; & \frac{k^4}{12\pi^2}\left[\frac{1}{\omega_{1,k}}\left(1+2n_B(\omega_{1,k}\right)+\frac{1}{\omega_{2,k}}\left(1+2n_B(\omega_{2,k}\right)\right] \\
& +\frac{|qB|}{2\pi^2}\sum_{m=0}^{\infty}\frac{k}{\omega_{1,k}}\sqrt{k^2-p_\perp^2(q,m,0)}\,\theta\left(k^2-p_\perp^2(q,m,0)\right) \\
& \times\left[1+2n_B(\omega_{1,k})\right] \\
& -\frac{N_c}{2\pi^2}\sum_{s,f,m=0}^{\infty}\frac{|q_fB|k}{\omega_{q,k}}\sqrt{k^2-p_\perp^2(q_f,m,s)} \\
& \times\theta\left(k^2-p_\perp^2(q_f,m,s)\right)\left[1-n_F^+(\omega_{q_f,k})-n_F^-(\omega_{q_f,k})\right]\;,
\end{aligned}
$$

Skokov, Phys. Rev. **D** 85 (2012) 034026

- Flow equation depends on regulator.

Functional renormalization group

- Boundary condition

$$\Gamma_{k=\Lambda}[\phi] = S_{\rm classical}\;,$$
$$S_{\rm classical} = \int d^4x\left[\frac{1}{2}m_\Lambda^2\phi^2+\frac{\lambda_\Lambda}{24}\phi^4\right]\;.$$

- m_Λ^2 and λ_Λ tuned to reproduce vacuum physics $T=B=0$ for $k=0$

$$m_{k,\pi}^2 = \left.\frac{\partial\tilde{U}_k}{\partial\rho}\right|_{\phi=\phi_k}\;,$$
$$m_{k,\sigma}^2 = m_{k,\pi}^2+2\rho\left.\frac{\partial^2\tilde{U}_k}{\partial\rho^2}\right|_{\phi=\phi_k}\;.$$

$$\left.\frac{\partial\tilde{U}_k}{\partial\phi}\right|_{\phi=\phi_k} = h\;,$$

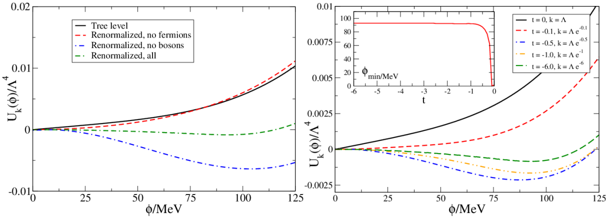

Figure: Effective potential in different approximations (left) and different $t = \ln \frac{k}{\Lambda}$.

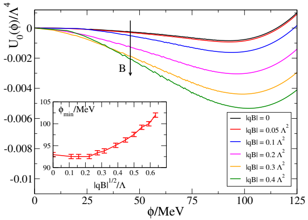

Figure: Effective potential for different values of B.

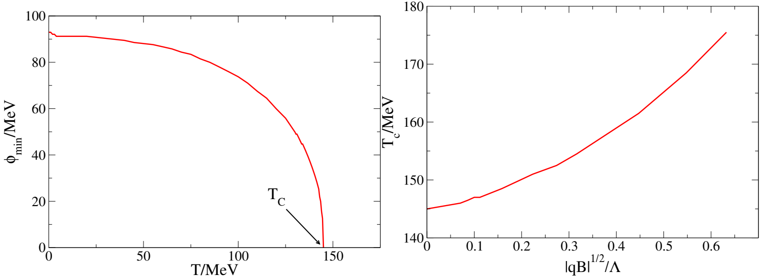

Figure: Order parameter $\phi(T)$ (left) and $T_c(B)$ (right).

Adding the Polyakov loop

- Polyakov loop Φ is an order parameter for confinement in (pure-glue) QCD

$$\begin{aligned}
\Phi &= \frac{1}{N_c}\mathrm{Tr}\langle L\rangle \\
L &= \mathcal{P}e^{i\int_0^\beta d\tau A_0(x,\tau)}\,. \\
\langle\Phi\rangle &\sim 0\,,\text{confinement at low}\,T\,, \\
\langle\Phi\rangle &\sim 1\,,\text{confinement at high}\,T\,.
\end{aligned}$$

- Adding the Polyakov loop by introducing a constant background A_0 [6]

$$\partial_\mu \rightarrow \partial_\mu - i\delta_{0\mu}A_\mu\,.$$

[6] Fukushima 2003.

- Distribution function

$$N_F \rightarrow \frac{1 + 2\Phi e^{\beta E_q} + \Phi e^{2\beta E_q}}{1 + 3e^{\beta E_q} + 3\Phi e^{2\beta E_q} + e^{3\beta E_q}} .$$

- Limits

$$N_F \rightarrow \frac{1}{e^{3\beta E_q} + 1} , \qquad \Phi = 0 .$$

$$N_F \rightarrow \frac{1}{e^{\beta E_q} + 1} , \qquad \Phi = 1 .$$

- Pure-glue potential

$$\frac{\mathcal{U}}{T^4} = -\frac{1}{2} a(T)\Phi^2 + b(t)\ln[1 - 6\Phi^2 + 8\Phi^3 - 3\Phi)^4] .$$

- $a(T)$ and $b(t)$ used to reproduce pure-glue QCD thermodyanmics. Other potentials with similar properties exist.

- Transition temperature T_0

$$a(T) \quad = \quad 3.51 - 2.47\left(\frac{T_0}{T}\right)^2 + 15.2\left(\frac{T_0}{T}\right)^3 \; .$$

- Make T_0 dependent of N_f to include backreaction from fermions.

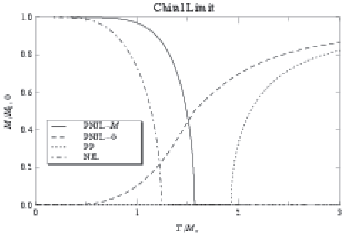

Figure: Quark condensate and Polyakov loop two-color QCD.

- Coupled equation for ϕ and Φ.
- QM and PQM model the same at $T = 0$.
- Less magnetic catalysis at finite temperature.
- Deconfinement transition hardly affected by B.

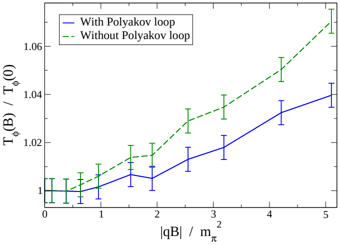

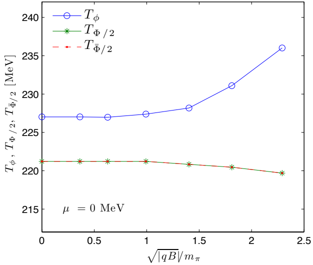

Lattice calculations

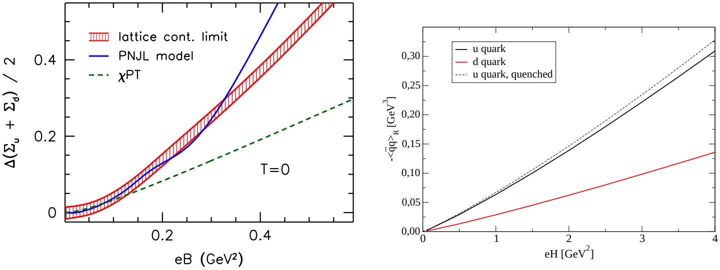

Figure: Quark condensates at $T = 0$. Bali et al 2012 (left) and Bonnet 2014 (right).

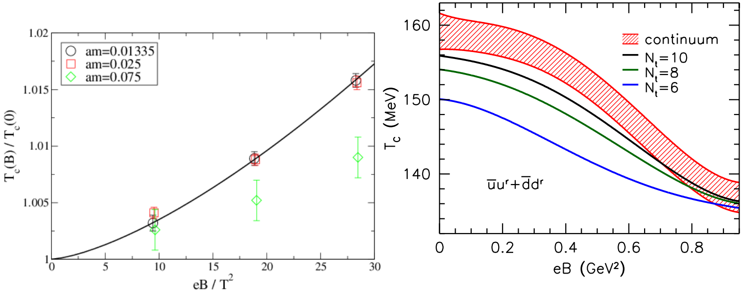

Figure: T_c as a function of the magnetic field B. D'Elia et al 2010 (left) and Bali et al 2012 (right).

$$\begin{aligned}
\mathcal{Z}(B) &= \int d\mathcal{U} e^{-S_g} \det(\not{D}(B) + m) \;, \\
\langle\bar{\psi}\psi\rangle &= \frac{1}{\mathcal{Z}(B)} \int d\mathcal{U} e^{-S_g} \det(\not{D}(B) + m) \mathrm{Tr}(\not{D}(B) + m)^{-1} \;,
\end{aligned}$$

- Valence contribution:

$$\langle\bar{\psi}\psi\rangle^{\text{val}} = \frac{1}{\mathcal{Z}(0)} \int d\mathcal{U} e^{-S_g} \det(\not{D}(0) + m) \mathrm{Tr}(\not{D}(B) + m)^{-1} \;.$$

- Sea contribution:

$$\langle\bar{\psi}\psi\rangle^{\text{sea}} = \frac{1}{\mathcal{Z}(B)} \int d\mathcal{U} e^{-S_g} \det(\not{D}(B) + m) \mathrm{Tr}(\not{D}(0) + m)^{-1} \;.$$

- Relative increment

$$r = \frac{\langle\bar{\psi}\psi\rangle(B)}{\langle\bar{\psi}\psi\rangle(0)} - 1 \, .$$

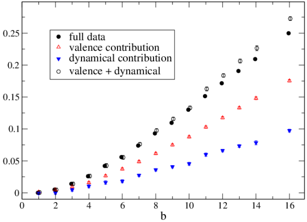

Figure: Valence and sea contribution to the quark condensate. D'Elia et al (2010).

- Banks-Casher relation

$$\lim_{V\to\infty}\lim_{m\to 0}\langle\bar{\psi}\psi\rangle \sim \lim_{V\to\infty}\lim_{m\to 0}\rho(\lambda)\,.$$

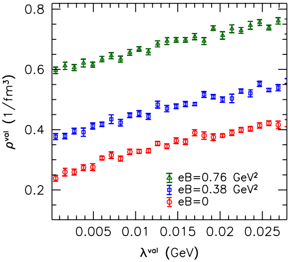

Figure: Spectral density for different values of B. Endrodi et al 2013.

- Reweighting

$$
\begin{aligned}
-\Delta S_f(B) &= \log\det(\not{D}(B)+m) - \log\det(\not{D}(0)+m) \\
\langle\bar{\psi}\psi\rangle &= \frac{\langle e^{-\Delta S_f(B)}\mathrm{Tr}(\not{D}(B)+m)^{-1}\rangle_0}{\langle e^{-\Delta S_f(B)}\rangle_0},
\end{aligned}
$$

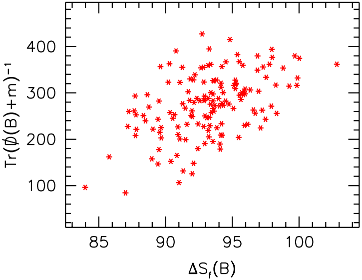

Figure: Scatter plot quark condensate as a function of $\Delta S(B)$. Endrodi et al 2013.

Model calculations revisited

- B-dependent coupling constant - QCD inspired

$$
\begin{aligned}
G(B) &= \frac{G_0}{1+\alpha \ln\left(1+\beta\frac{|qB|}{\Lambda_{\rm QCD}}\right)}\,, \\
G(B,T) &= G(B)\left(1-\gamma\frac{|qB|}{\Lambda_{\rm QCD}^2}\frac{T}{\Lambda_{\rm QCD}}\,.\right)
\end{aligned}
$$

- Fit parameters to reproduce quark condensate at $T=0$ and at high T.

Model calculations revisited

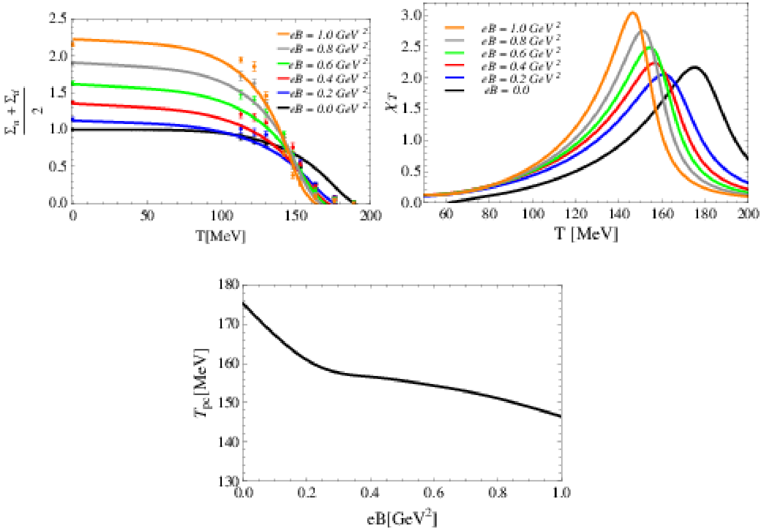

Figure: Farias (2014).

Conclusions and Outlook

- Order of phase transition depends on treatment of vacuum fluctuations - take them seriously.
- Functional RG predicts a second order transition
- Model calculations correctly predict magnetic catalysis at $T = 0$, but fail to reproduce inverse magnetic catalysis around the transition temperature.
- Some model calculations have been modified to reproduce lattice results - essentially curve fitting.
- Need to incorporate back-reaction from fermion determinant.